



Cite this: *Nanoscale*, 2020, **12**, 785

Predictive theoretical screening of phase stability for chemical order and disorder in quaternary 312 and 413 MAX phases†

Martin Dahlqvist * and Johanna Rosen*

In this work we systematically explore a class of atomically laminated materials, $M_{n+1}AX_n$ (MAX) phases upon alloying between two transition metals, M' and M'' , from groups III to VI (Sc, Y, Ti, Zr, Hf, V, Nb, Ta, Cr, Mo, W). The materials investigated focus on so called o-MAX phases with out-of-plane chemical ordering of M' and M'' , and their disordered counterparts, for $A = \text{Al}$ and $X = \text{C}$. Through use of predictive phase stability calculations, we confirm all experimentally known phases to date, and also suggest a range of stable ordered and disordered hypothetical elemental combinations. Ordered o-MAX is favoured when (i) M' next to the Al-layer does not form a corresponding binary rock-salt MC structure, (ii) the size difference between M' and M'' is small, and (iii) the difference in electronegativity between M' and Al is large. Preference for chemical disorder is favoured when the size and electronegativity of M' and M'' is similar, in combination with a minor difference in electronegativity of M' and Al. We also propose guidelines to use in the search for novel o-MAX; to combine M' from group 6 (Cr, Mo, W) with M'' from groups 3 to 5 (Sc only for 312, Ti, Zr, Hf, V, Nb, Ta). Correspondingly, we suggest formation of disordered MAX phases by combining M' and M'' within groups 3 to 5 (Sc, Ti, Zr, Hf, V, Nb, Ta). The addition of novel elemental combinations in MAX phases, and in turn in their potential two-dimensional MXene derivatives, allow for property tuning of functional materials.

Received 9th October 2019,
Accepted 3rd December 2019

DOI: 10.1039/c9nr08675g

rsc.li/nanoscale

Introduction

In the 1960s a family of atomically laminated ternary carbide and nitride materials was discovered.^{1,2} In the 1990s, these so-called MAX phases gained renewed attention when shown to combine metallic and ceramic attributes like high electric and thermal conductivity, machinability, oxidation resistance, and high temperature mechanical properties.^{3,4} The MAX phases are of the general formula $M_{n+1}AX_n$ ($n = 1-3$), where $M_{n+1}X_n$ sheets, based on a transition metal M and X as C or N, are interleaved by one atom thick A-layers (A is an A-group element). A short notion typically used to describe MAX phases are 211, 312, and 413, depending on the value of n being 1, 2, and 3, respectively. MAX phases are important as parent materials for their two-dimensional (2D) derivative, MXene, realized from selective etching of the A-element.^{5,6} MXenes show promise for a wide range of applications,

including energy storage and electromagnetic interference shielding.^{7,8}

A common route for property tuning is through alloying, which for MAX phases can be realized with a fourth element on either M, A, or X site, as demonstrated to change *e.g.* hardness,⁹ to tune properties for isotropic thermal expansion,¹⁰ and to introduce magnetic characteristics.¹¹ Traditionally, MAX phase alloys have to a large extent been disordered solid solutions with challenges in attaining an exact *a priori* composition.¹² However, in 2014 Liu *et al.* synthesized a chemically ordered 312 MAX phase, $\text{Cr}_2\text{TiAlC}_2$,¹³ defined by out-of-plane ordering through alternating M-layers based on one M-element only, later coined o-MAX. This was soon followed by other out-of-plane ordered phases, $\text{Mo}_2\text{TiAlC}_2$,^{14,15} $\text{Mo}_2\text{ScAlC}_2$,¹⁶ $\text{Cr}_{1.5}\text{V}_{1.5}\text{AlC}_2$,¹⁷ and corresponding 413 in the form of $\text{Mo}_2\text{Ti}_2\text{AlC}_3$ and $\text{Cr}_2\text{V}_2\text{AlC}_3$.^{15,17} Common for o-MAX phases are the two crystallographic different M-sites, with Wyckoff positions $4f$ (M') and $2a$ (M'') for 312 and $4f$ (M') and $4e$ (M'') for 413. This is opposed to the most recent discovery of a family of in-plane ordered 211 MAX phase related materials, coined i-MAX, where the two metals have a 2 : 1 ratio within each metal layer.¹⁸⁻²³

Chemically ordered o-MAX and i-MAX phases are highly interesting as they allow for incorporation of non-traditional

Thin Film Physics, Department of Physics, Chemistry and Biology (IFM) Linköping University, SE-581 83 Linköping, Sweden. E-mail: martin.dahlqvist@liu.se, johanna.rosen@liu.se

†Electronic supplementary information (ESI) available. See DOI: 10.1039/c9nr08675g



MAX phase elements, *e.g.*, Sc,^{16,18,23} Y,^{19,21,23} and W,²² but also for the improved control of the alloy composition. However, there has been no extensive systematic study in the quest for yet hypothetical ordered MAX phases other than for Ti-based o-MAX.²⁴ In this work we focus on alloying between two metals, M' and M'', in quaternary 312 and 413 o-MAX phases, to systematically explore chemically ordered (out-of-plane) and disordered distributions of M' and M'' with M elements from groups 3 to 6 (Sc, Y, Ti, Zr, Hf, V, Nb, Ta, Cr, Mo, and W) while keeping A and X equal to Al and C, respectively. The A = Al choice is motivated by Al being prone to chemical etching for MXene derivation, as shown for the o-MAX phases Cr₂TiAlC₂, Mo₂TiAlC₂, Mo₂ScAlC₂, and Mo₂Ti₂AlC₃.^{16,25}

This study on o-MAX phases is structured into two parts, starting with predictive stability calculations for chemically ordered and disordered distributions of M' and M''. We confirm the stability of the quaternary phases reported to date, and also suggest several ordered as well as disordered novel alloys yet to be experimentally discovered. In the second part, we investigate the impact of choice of element M' and M'', and effect of size and electronegativity of M', M'' and Al, for the formation of chemically ordered (o-MAX) or disordered MAX phases. We also propose guidelines for which elemental combinations to use in search for novel o-MAX phases, by combining M' and M'' from specific groups, and how to promote chemical order *vs.* disorder.

Method

All first-principles calculations were performed by means of density functional theory (DFT) and the projector augmented wave method,^{26,27} as implemented within the Vienna *ab initio* simulation package (VASP) version 5.4.1.^{28–30} We used the non-spin polarized generalized gradient approximation (GGA) as parameterized by Perdew–Burke–Ernzerhof (PBE) for treating the electron exchange and correlation effects.³¹ For Cr-based phases we used the spin-polarized version with multiple spin

configurations considered within the unit cell in line with ref. 24. Presented results are for the lowest energy spin configuration. We also used a plane-wave energy cut-off of 400 eV, and the Monkhorst–Pack scheme for sampling of the Brillouin zone.³² The total energy is minimized through relaxation of the unit-cell shape and volume, and internal atomic positions.

In this work we assume the o-MAX chemical order with the notation of M' facing the Al-layer, while M'' is being sandwiched between carbon layers in the 312 and 413 MAX phase structures. For 312 this corresponds to a 2:1:1:2 composition of M':M'':Al:C with M' at 4*f* and M'' at 2*a* Wyckoff positions, and for the 413 this corresponds to a 2:2:1:3 composition of M':M'':Al:C with M' at 4*f* and M'' at 4*e* Wyckoff positions. In addition, for the 312 MAX phase, five semi-ordered structures have been modelled, with a 2:1:1:2 composition of M':M'':Al:C, as shown in Fig. 1a. For the 413 MAX phase, a total of 22 unique ordered structures have been modelled within the unit cell, with a 2:2:1:3 composition of M':M'':Al:C, as shown in Fig. S1.† Four selected configurations are shown in Fig. 1b. Note that the o-MAX structure has previously been shown to be dynamically stable.^{33,34} In the present work we considered M' and M'' from groups 3 to 6; Sc, Y, Ti, Zr, Hf, V, Nb, Ta, Cr, Mo, and W. To model chemical disorder of M' and M'' on the M sublattices we used the special quasi-random structure (SQS) method³⁵ with supercell sizes of 4 × 4 × 1 unit cells, *i.e.* 192 and 256 atoms for the 312 and 413 MAX phases, respectively. Convergence tests show that the supercells used give a qualitatively accurate representation and a quantitative convergence in terms of calculated formation enthalpies, equilibrium volumes, and lattice parameters.

The thermodynamic stability of quaternary MAX phases is investigated at 0 K with respect to decomposition into any combination of competing phases. The most competing set of competing phases, denoted equilibrium simplex, is identified using a linear optimization procedure^{36,37} which have been proven successful to confirm already experimentally known MAX phases as well as predicting the existence of new ones.^{11,37–41} The stability of the quaternary MAX phase is

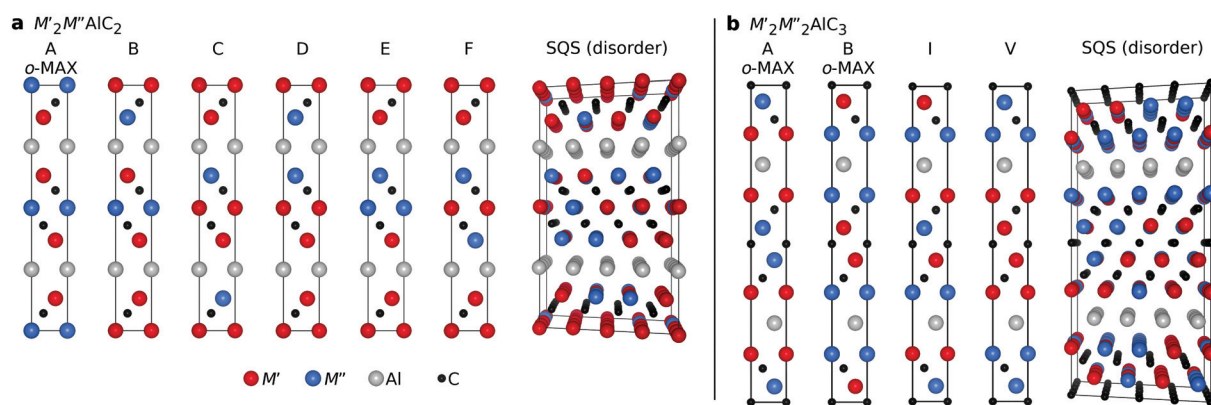


Fig. 1 Schematic illustration of considered chemical order of M' and M'' for (a) a 312 MAX phase structure with a 2:1:1:2 composition of M':M'':Al:C and (b) a 413 MAX phase structure with a 2:2:1:3 composition of M':M'':Al:C, where M', M'', Al, and C atoms are represented in red, blue, grey, and black, respectively. In (b), only selected structures are shown for the 413 MAX phase, for further details see Fig. S1.†



quantified in terms of formation enthalpy ΔH_{cp} by comparing its energy to the energy of the equilibrium simplex according to

$$\Delta H_{\text{cp}} = E(\text{MAX}) - E(\text{equilibrium simplex}). \quad (1)$$

A phase is concluded stable when $\Delta H_{\text{cp}} < 0$. Here $E(\text{MAX})$ represent the chemically ordered or disordered MAX phase structure of lowest energy. However, when $T \neq 0$ K, the contribution from configurational entropy due to disorder of M' and M'' on the M sublattices will decrease the Gibbs free energy $\Delta G_{\text{cp}}^{\text{disorder}}$ as approximated by

$$\Delta G_{\text{cp}}^{\text{disorder}}[T] = \Delta H_{\text{cp}}^{\text{disorder}} - T\Delta S, \quad (2)$$

where the entropic contribution ΔS , assuming an ideal solution of M' and M'' on the M-sites, is given by

$$\Delta S = -2k_{\text{B}}[z \ln(z) + (1-z)\ln(1-z)], \quad (3)$$

where k_{B} is the Boltzmann constant and z is the concentration of M'' on the M-sublattices. By combining eqn (1) and (2), a disorder temperature T_{disorder} can be calculated according to

$$T_{\text{disorder}} = \frac{\Delta H_{\text{cp}}^{\text{disorder}} - \Delta H_{\text{cp}}^{\text{order}}}{\Delta S}, \quad (4)$$

for which $\Delta G_{\text{cp}}^{\text{disorder}}[T] = \Delta H_{\text{cp}}^{\text{order}}$ is fulfilled. This gives an estimate of above which temperature chemical disorder is expected. The temperature can then be compared to the experimental conditions used, e.g., typical bulk synthesis temperatures of 1200–1600 °C (1473–1873 K).

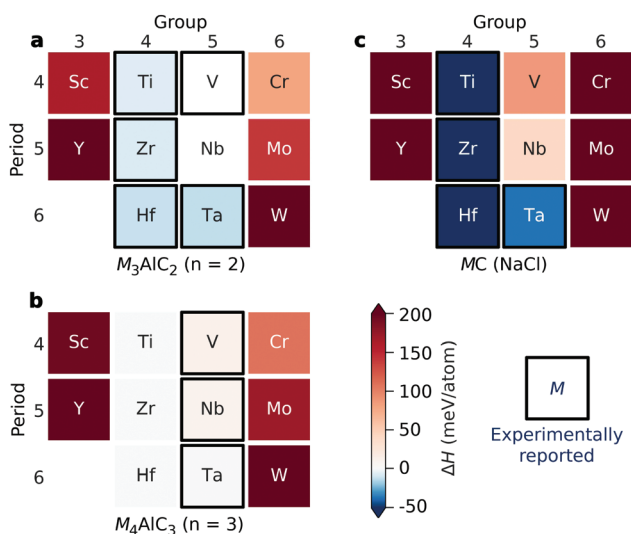


Fig. 2 Calculated formation enthalpy ΔH_{cp} for (a) M_3AlC_2 and (b) M_4AlC_3 MAX phases, and (c) binary MC in its rock-salt structure (NaCl). Blue indicates a stable phase and red metastable versus the set of most competing phases. Experimentally reported phases are marked by a black square.

Results and discussion

Stability of ternary 312 and 413 MAX phases

We start by investigating the thermodynamic stability of the ternary M_3AlC_2 and M_4AlC_3 MAX phases. Fig. 2 shows the calculated formation enthalpy ΔH_{cp} at 0 K for both M_3AlC_2 ($n=2$) and M_4AlC_3 ($n=3$), with corresponding identified equilibrium simplex listed in Tables S1 and S2.† Thermodynamically stable, or close to stable, MAX phases with $n=2$ and 3 are found for M from groups 4 and 5, while MAX phases with M from groups 3 and 6 are far from stable. Experimentally known phases are all identified as stable or close to stable ($H_{\text{cp}} < +12$ meV per atom). In addition, Nb_3AlC_2 and M_4AlC_3 ($M = \text{Ti, Zr, Hf}$) are also predicted to be stable MAX phases ($\Delta H_{\text{cp}} < 0$) but are yet to be experimentally discovered. Note that all four

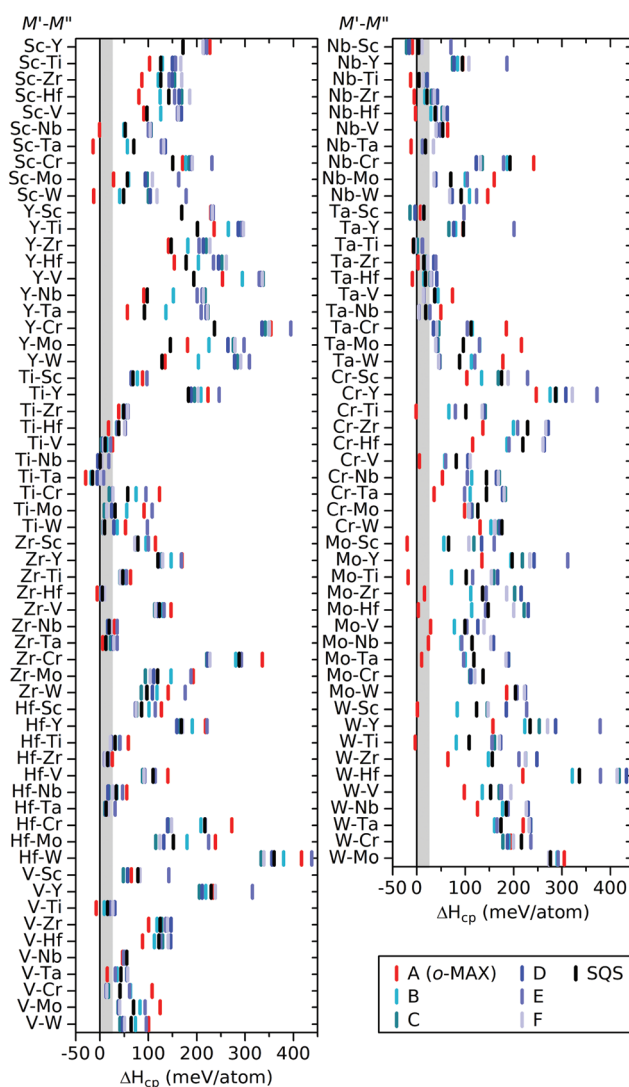


Fig. 3 Calculated formation enthalpy ΔH_{cp} of the 312 MAX phase structures with a 2:1:1:2 composition of $M':M'':Al:C$, for six chemically ordered (A to F, as shown in Fig. 1a) and one chemically disordered (SQS) distribution of M' and M'' . The grey area represents $0 \leq \Delta H_{\text{cp}} \leq 25$ and includes those phases which are close to stable.



of these stable hypothetical MAX phases are competing with the formation of other known MAX phases, as indicated in Tables S1 and S2.†

The trends in thermodynamic stability for both M_3AlC_2 and M_4AlC_3 is similar to the trends found for the binary MC phase in its rock salt structure (see Fig. 2c), where M from groups 4 (Ti, Zr, Hf) and 5 (V, Nb, Ta) is found to be stable or close to stable while M from groups 3 (Sc, Y) and 6 (Cr, Mo, W) is far from stable ($\Delta H_{cp} > +200$ meV per atom). The comparable trends can be related to the stacking of M and C in the $M_{n+1}C_n$ layers of the MAX phases which is also found along the 111 direction of rock salt MC.

Order and disorder in quaternary 312 MAX phases

For each 2 : 1 : 1 : 2 composition of $M' : M'' : Al : C$ (M' and $M'' = Sc, Y, Ti, Zr, Hf, V, Nb, Ta, Cr, Mo, W$) we solve the linear optimization problem and identify the equilibrium simplex, see Table S3,† and its corresponding ΔH_{cp} and $T_{disorder}$. Fig. 3 shows ΔH_{cp} for different chemical ordering; six ordered (A to F, depicted in Fig. 1a) and one disordered (SQS). The spread in ΔH_{cp} among the considered chemical order configurations is rather small for some systems, e.g. Ti- M'' and V- M'' , while others show much larger variation, e.g. Cr- M'' and Mo- M'' .

The long list in Fig. 3 of ΔH_{cp} for 110 compositions represented with different configurations of chemical order does not provide a clear picture of whether chemical order or disorder are to be preferred at typical synthesis conditions. In Fig. 4, we therefore visualize the trends in thermodynamic stability using a heatmap, where M' and M'' are sorted according to the periodic group in which the metal lies. The background colour represents the calculated thermodynamic stability for chemical order of lowest energy, with a blue region representing stable phases (ΔH_{cp} or $\Delta G_{cp} < 0$). We also use a symbol representation to denote the type of chemical order of lowest energy. In addition, experimentally known MAX phases

are marked by a square, where the colour represent the type of reported chemical order. Fig. 4a depicts the calculated formation enthalpy at 0 K, showing that the vast majority of M' and M'' combinations are chemically ordered, with 55 o-MAX (filled squares) and 45 of order B to F (filled triangles). Reported o-MAX phases to date are identified as stable; Cr_2TiAlC_2 ,¹³ Mo_2ScAl_2 ,¹⁶ and Mo_2TiAlC_2 .¹⁴ However, the result obtained at 0 K do not capture the MAX phases reported with disorder between M' and M'' ; $(Zr_{0.67}Ti_{0.33})_3AlC_2$,⁴² $(V_{0.67}Ti_{0.33})_3AlC_2$,⁴³ and $(Nb_{0.67}Sc_{0.33})_3AlC_2$.⁴⁴

Since typical bulk synthesis of MAX phase are performed around 1773 K we need to consider the contribution from configurational entropy to the Gibbs free energy, using eqn (2) and (3) for structures with disordered distribution of M' and M'' (SQS). Fig. 4b depicts either the calculated formation enthalpy ΔH_{cp} (for ordered phases) or Gibbs free energy of formation ΔG_{cp} at 1773 K (for disordered phases), depending on which order is of lowest energy. In such a representation, 79 out of 110 M' and M'' combinations are identified as disordered, and out of these 28 are stable, including the MAX phases reported to date with disorder on M-sublattices. Furthermore, 31 phases are identified as o-MAX, with 7 being stable, including those reported experimentally; Cr_2TiAlC_2 ,¹³ Mo_2ScAl_2 ,¹⁶ and Mo_2TiAlC_2 .¹⁴ For Cr_2VAlC_2 , we find the o-MAX to be of lowest energy, with $\Delta H_{cp} = 6$ meV per atom, and it has indeed been synthesized, albeit with some intermixing of V on the Cr site (M'), $(Cr_{0.75}V_{0.25})_2VAlC_2$.¹⁷ For $M' = Ti$ and $M'' = Zr$, both Ti_2ZrAlC_2 o-MAX and disordered $(Ti_{0.67}Zr_{0.33})_3AlC_2$ have been reported.^{42,45} Our theoretical results indicate that disorder is preferred, though a more in-depth discussion of these discrepancies will be presented below.

Beyond the phases reported to date, we predict four stable o-MAX phases; Sc_2NbAlC_2 , Sc_2TaAlC_2 , Sc_2WAlC_2 , and W_2TiAlC_2 . An additional six o-MAX phases are close to stable; $Mo_2M''AlC_2$ ($M'' = Zr, Hf, V, Nb, Ta$) and W_2ScAlC_2 . We also

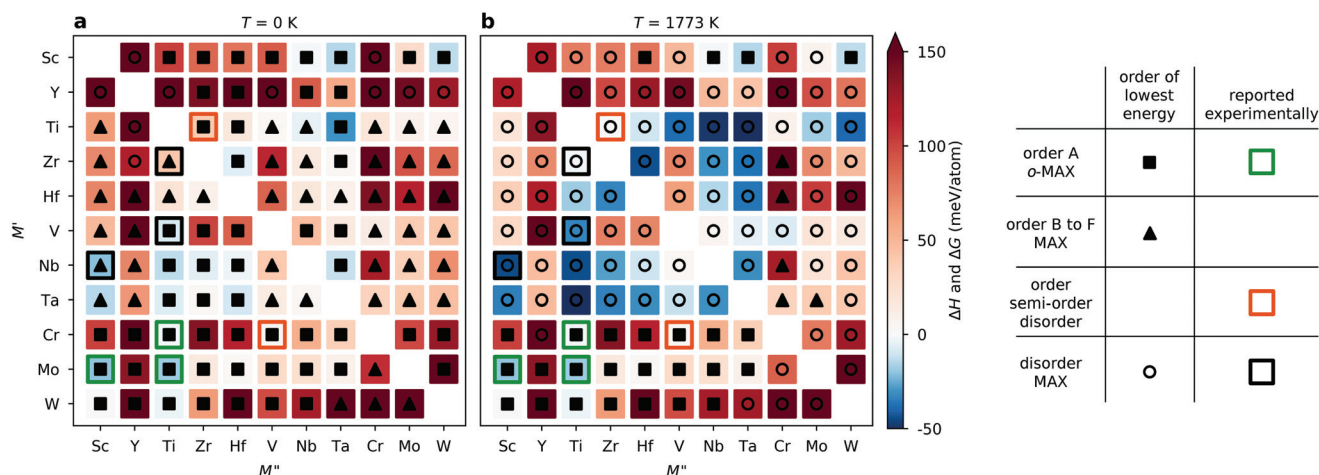


Fig. 4 Summary of the stability for 312 MAX phase structures with a 2 : 1 : 1 : 2 composition of $M' : M'' : Al : C$ indicating if chemical order (filled squares for o-MAX and filled triangles for order B to F) or disorder (open circles) is preferred at (a) 0 K and (b) at a typical synthesis temperature of 1773 K. In addition, experimentally reported phases are marked by open squares where its colour indicates reported order; green (o-MAX), orange (o-MAX, semi-order, or disorder), and black (disorder MAX).



identify 26 systems which are stable, though with a preference for disorder at $T < 1773$ K, with most of these phases combining M' and M'' from groups 4 and 5.

Order and disorder in 413 MAX phases

Identification of the equilibrium simplex was made for each 2:2:1:3 composition of $M':M'':Al:C$ (M' and $M'' = Sc, Y, Ti, Zr, Hf, V, Nb, Ta, Cr, Mo, and W$), see Table S3.† The formation enthalpy ΔH_{cp} , calculated using eqn (1), is shown in Fig. 5 for different chemical ordering; two ordered o-MAX (A and B), order of type I and V (see Fig. 1b), an additional 18 ordered structures (other), and one disordered (SQS). A schematic illustration of the 22 ordered structures is shown in Fig. S1.† Note that B is the inverse of A, and hence doublets are found, e.g., $Mo_2Ti_2AlC_3$ of type A is equal to $Ti_2Mo_2AlC_3$ of type B. The spread in ΔH_{cp} between the considered configurations is more pronounced than for the 312 systems, but shows a similar overall trend with less spread in energies for certain systems, e.g. Ti- M'' , while others show a much larger spread, e.g. Mo- M'' .

Again, we use a heatmap representation to visualize the thermodynamic stability and to determine whether chemical order or disorder is preferred at 0 K and at typical synthesis conditions (1773 K). Fig. 6a depicts ΔH_{cp} at 0 K showing that a majority, 41 of 55, of the M' and M'' combinations are ordered in the o-MAX structure. Reported o-MAX phases to date are identified as stable, $Mo_2Ti_2AlC_3$,¹⁵ or close to stable for $Cr_2Ti_2AlC_3$ and $Cr_2V_2AlC_3$.^{17,46} 11 combinations show preference for order of type I and only 3 show preference for disorder. Again, the reported disordered MAX phases are not captured by the 0 K results, and we therefore consider the contribution from the configurational entropy to the Gibbs free energy, using eqn (2) and (3), at a typical bulk synthesis temperature of 1773 K. Fig. 6b depicts the calculated ΔH_{cp} (for o-MAX phases) or ΔG_{cp} at 1773 K (for disordered MAX phases), depending on which ordering is of lowest energy. Now 32 out of 55 M' and M'' combinations are identified as disordered, and out of these 13 are predicted stable, including the MAX phases reported to date with disorder; $(Ti_{0.5}Nb_{0.5})_4AlC_3$,⁴⁷ $(V_{0.5}Cr_{0.5})_4AlC_3$,⁴⁸ and $(Nb_{0.5}V_{0.5})_4AlC_3$.⁴³ $(Nb_{0.5}Sc_{0.5})_4AlC_3$ is one of the concluded stable disordered phases, and a chemically related phase, $(Nb_{0.67}Sc_{0.33})_4AlC_3$, has recently been synthesized, albeit with a diverging stoichiometry compared to herein.⁴⁴ 23 phases are identified as o-MAX, with 4 being predicted stable, including the experimentally reported $Mo_2Ti_2AlC_3$.¹⁵

Beyond the reported o-MAX we here predict three phases to be stable with preference for o-MAX ordering; $Nb_2Hf_2AlC_3$, $Mo_2Ta_2AlC_3$, and $W_2Ti_2AlC_3$. An additional four systems are close to stable with preference for o-MAX ordering; $Cr_2Ta_2AlC_3$, $Mo_2Zr_2AlC_3$, $Mo_2Hf_2AlC_3$ and $Mo_2Nb_2AlC_3$. We also identify 12 systems which are stable and with preference for disorder at $T = 1773$ K, with a majority combining M' and M'' from groups 4 and 5.

Table 1 summarizes selected key results of the thermodynamic stability evaluation, where stable and close to stable

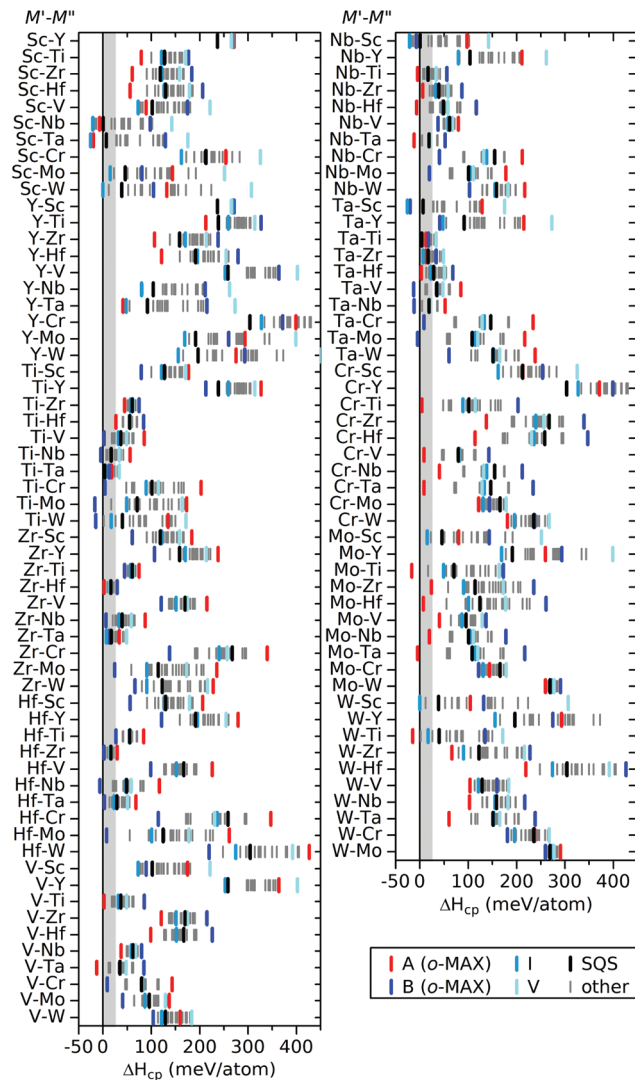


Fig. 5 Calculated formation enthalpy ΔH_{cp} of the 413 MAX phase structures with a 2:2:1:3 composition of $M':M'':Al:C$, for chemically ordered o-MAX (A and B), order of type I and V (shown in Fig. 1b), additional (other) ordered configurations, and chemically disordered (SQS) configurations of M' and M'' .

312 and 413 MAX phases with their preference for order or disorder are given. Comparing the experimentally reported phases and their calculated stability, the results are consistent. In addition, we also list hypothetical phases that are stable or close to stable, and provide information on whether or not chemical order or disorder of M' and M'' is to be expected.

The origin of out-of-plane chemical order and disorder in MAX phases

Previous studies of o-MAX phases claim that metals like Mo and Cr tend to avoid the unfavourable fcc stacking with C, whereas elements like Ti prefer such arrangement.^{15,24,25} It has also been shown that for the hypothetical Mo_3AlC_2 , the traditional MAX phase structure with fcc arrangement of Mo and C is not lowest in energy ($\Delta H_{cp} = +141$ meV per atom). Instead,



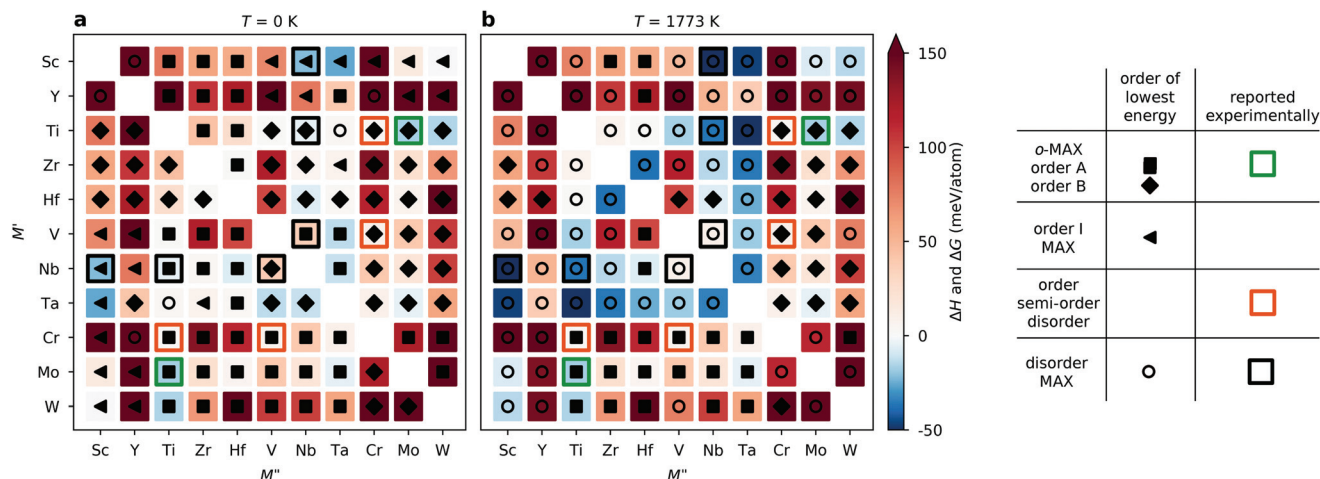


Fig. 6 Summary of stability for 413 MAX phase structures with a 2 : 2 : 1 : 3 composition of $M' : M'' : Al : C$, indicating if chemical order (filled symbols) or disorder (open circles) is preferred at (a) 0 K and (b) at a typical synthesis temperature of 1773 K. In addition, experimentally reported phases are marked by an open square where its colour indicates reported order; green (o-MAX), black (disorder MAX), and orange (o-MAX, semi-order, or disorder).

Table 1 Experimentally reported and theoretically predicted quaternary MAX phases, categorized by the calculated thermodynamic stability and their preference for ordered (o-MAX) or disordered distribution of M' and M'' at a typical synthesis temperature. The unit for ΔH_{cp} is in meV per atom

Phase	Stability criteria	Experimentally reported and here predicted	Predicted
o-MAX stable	$\Delta H_{cp} < 0$ $T_{\text{disorder}} > 1773 \text{ K}$	$\text{Cr}_2\text{TiAlC}_2$ ¹³ Mo_2ScAl_2 ¹⁶ $\text{Mo}_2\text{TiAlC}_2$ ¹⁴ $\text{Mo}_2\text{Ta}_2\text{AlC}_3$ ¹⁵	$\text{Sc}_2M''\text{AlC}_2$, ($M'' = \text{Nb, Ta, W}$) W_2TiAlC_2 $\text{Nb}_2\text{Hf}_2\text{AlC}_3$ $\text{Mo}_2\text{Ta}_2\text{AlC}_3$ $\text{W}_2\text{Ti}_2\text{AlC}_3$
o-MAX close to stable	$0 \leq \Delta H_{cp} < +50$ $T_{\text{disorder}} > 1773 \text{ K}$	Cr_2VAlC_2 ^{17 a} $\text{Cr}_2\text{Ti}_2\text{AlC}_3$ ^{46 b} $\text{Cr}_2\text{V}_2\text{AlC}_3$ ^{17 c}	$\text{Mo}_2M''\text{AlC}_2$ ($M'' = \text{Zr, Hf, V, Nb, Ta}$) W_2ScAlC_2 $\text{Cr}_2\text{Ta}_2\text{AlC}_3$ $\text{Mo}_2M''_2\text{AlC}_3$ ($M'' = \text{Zr, Hf, Nb}$)
Disordered MAX	$\Delta G_{cp}[1773 \text{ K}] \leq 0$ $T_{\text{disorder}} < 1773 \text{ K}$	$(\text{Zr}_{0.67}\text{Ti}_{0.33})_3\text{AlC}_2$ ⁴² $(\text{Ti}_{0.67}\text{Zr}_{0.33})_3\text{AlC}_2$ ^{42 d} $(\text{V}_{0.67}\text{Ti}_{0.33})_3\text{AlC}_2$ ⁴³ $(\text{Nb}_{0.67}\text{Sc}_{0.33})_3\text{AlC}_2$ ⁴⁴ $(\text{Ti}_{0.5}\text{Nb}_{0.5})_4\text{AlC}_3$ ⁴⁷ $(\text{V}_{0.5}\text{Cr}_{0.5})_4\text{AlC}_3$ ⁴⁸ $(\text{Nb}_{0.5}\text{V}_{0.5})_4\text{AlC}_3$ ⁴³ $(\text{Nb}_{0.5}\text{Sc}_{0.5})_4\text{AlC}_3$ ^{44 e}	$(\text{Ti}_{0.67}M''_{0.33})_3\text{AlC}_2$ ($M'' = \text{Hf, V, Nb, Ta, Mo, W}$) $(\text{Zr}_{0.67}M''_{0.33})_3\text{AlC}_2$ ($M'' = \text{Hf, Nb, Ta}$) $(\text{Hf}_{0.67}M''_{0.33})_3\text{AlC}_2$ ($M'' = \text{Ti, Zr, Nb, Ta}$) $(\text{V}_{0.67}M''_{0.33})_3\text{AlC}_2$ ($M'' = \text{Ta, Cr}$) $(\text{Nb}_{0.67}M''_{0.33})_3\text{AlC}_2$ ($M'' = \text{Ti, Zr, Hf, Ta}$) $(\text{Ta}_{0.67}M''_{0.33})_3\text{AlC}_2$ ($M'' = \text{Sc, Ti, Zr, Hf, V, Nb}$) $(\text{Sc}_{0.5}M''_{0.5})_4\text{AlC}_3$ ($M'' = \text{Ta, Mo, W}$) $(\text{Ti}_{0.5}M''_{0.5})_4\text{AlC}_3$ ($M'' = \text{V, Ta}$) $(\text{Zr}_{0.5}M''_{0.5})_4\text{AlC}_3$ ($M'' = \text{Hf, Nb, Ta}$) $(\text{Hf}_{0.5}M''_{0.5})_4\text{AlC}_3$ ($M'' = \text{Nb, Ta}$) $(\text{Ta}_{0.5}M''_{0.5})_4\text{AlC}_3$ ($M'' = \text{V, Nb}$)

^a Reported with intermixing of V on Cr-site $(\text{Cr}_{0.75}\text{V}_{0.25})_2\text{AlC}_2$. ^b Reported with slight off-stoichiometric $\text{Cr}_{2.5}\text{Ti}_{1.5}\text{AlC}_3$. ^c Reported with some intermixing between M sublattices $(\text{Cr}_{0.7}\text{V}_{0.3})_2(\text{V}_{0.8}\text{Cr}_{0.2})_2\text{AlC}_3$. ^d Have also been reported as $\text{Ti}_2\text{ZrAlC}_2$ o-MAX. ^e Reported stoichiometry $(\text{Nb}_{0.67}\text{Sc}_{0.33})_4\text{AlC}_3$.

the Mo_3C_2 -layer prefers an ABAB stacking closely related to WC ($\Delta H_{cp} = +81$ meV per atom).²⁴ In some o-MAX phases, e.g., $\text{Mo}_2\text{TiAlC}_2$, the unfavourable fcc arrangement of Mo and C is broken by replacing Mo with Ti in the mid-layer (M'' at site 2a), resulting in $\Delta H_{cp} = -17$ meV per atom. However, this is not valid for all o-MAX phases, e.g., $\text{Mo}_2\text{ScAlC}_2$.¹⁶ An additional explanation is therefore that M' at site 4f, next to the Al layer, should be more electronegative than Al, resulting in fewer elec-

trons available for populating antibonding Al–Al orbitals, which is energetically expensive.²⁴

To increase the understanding of the formation of ordered and disordered MAX phase configurations, and to test the previously suggested hypothesis for the origin of o-MAX, we choose to investigate trends in type of metal M' next to the Al layer (site 4f for 312 and 413), type of metal M'' sandwiched between C layers (site 2a for 312 and 4e for 413), and the



metallic radius (r) and electronegativity (ρ) of M' , M'' and A. For this analysis, only chemical order of type A (o-MAX) and chemical disorder is considered.

We start by looking at whether the metals M' and M'' in o-MAX also prefer formation of the binary MC in its rock salt structure. To be consistent, we herein use ΔH_{cp} in the analysis instead of the isostructural formation enthalpy, ΔH_{iso} , since the latter is biased from whether M prefer an fcc arrangement with C or not. This is most pronounced for the 413 system as seen in Fig. S2.† In Fig. 7, the calculated ΔH_{cp} for o-MAX is shown as a function of the disorder temperature $T_{disorder}$, where the colouring represents if M' and/or M'' in the o-MAX structure also form the binary rock salt MC. Note that for $T_{disorder} < 0$, the disorderd MAX is lower in energy than o-MAX, whereas for $T_{disorder} > 0$, the o-MAX is lower in energy. In addition, experimentally reported phases have been marked according to their reported order to aid in the interpretation. For both 312 and 413 o-MAX phases qualitatively similar results are found;

- When both M' and M'' in o-MAX also form MC (red), this results in $T_{disorder}$ close to zero, *i.e.*, no or small energy difference between order and disorder, indicating preference for disorder at typical synthesis temperatures.
- When only M' in o-MAX also form MC (light red), this results in $T_{disorder} < 0$, *i.e.*, disorder is lower in energy than order, clearly indicating preference for disorder.
- When only M'' in o-MAX also form MC (light grey), this generally results in $T_{disorder} > 0$, *i.e.*, order is lower in energy than disorder at 0 K. When $T_{disorder} > 1773$ K, preference for o-MAX is expected.
- When none of M' and M'' in o-MAX form MC (dark grey) we find -5000 K $< T_{disorder} < +5000$ K. Hence, no general rule can be identified for this case.

The presented results partially support the previous statement that having a M'' that also form a rock-salt MC is beneficial for o-MAX formation ($\text{Cr}_2\text{TiAlC}_2$ and $\text{Mo}_2\text{Ti}_2\text{AlC}_3$), but this do not explain the formation of, *e.g.*, $\text{Mo}_2\text{ScAlC}_2$.

Trends in ΔH_{cp} for o-MAX as a function of the disorder temperature $T_{disorder}$ is shown in Fig. 8 for $M'_2M''\text{AlC}_2$ (left) and $M'_2M''_2\text{AlC}_3$ (right). The colouring in the top panels represent the difference in size between M' and M'' , where red represents $r_{M'} > r_{M''}$ and blue $r_{M'} < r_{M''}$. The mid panels display the difference in electronegativity between M' and M'' , where red represents $\rho_{M'} > \rho_{M''}$ and blue $\rho_{M'} < \rho_{M''}$, while the bottom panels display the difference in electronegativity between M' and Al, where red represents $\rho_{M'} > \rho_{Al}$ and blue $\rho_{M'} < \rho_{Al}$. The values used for r and ρ are found in Table S5.†

Focusing on the region which indicates a preference for chemical order, *i.e.*, $T_{disorder} > 1773$ K, suggests that for a majority of phases M' should be more electronegative than M'' and with a size difference of M' and M'' being at most 0.2 Å. We also find that M' should be more electronegative than Al. The latter is in line with previous work suggesting that having a M' with larger electronegativity than Al results in fewer electrons available for populating antibonding Al–Al orbitals.²⁴

Within the region where disorder is preferred, *i.e.*, $T_{disorder} < 1773$ K, and with $0 < \Delta H_{cp} < +50$ meV per atom, we find hypothetical as well as experimentally reported disordered phases, with a difference in electronegativity of M' and M'' within 0.4, while the size difference of M' and M'' does not exceed 0.2 Å. The results also indicate that the difference in electronegativity of M' and Al should be small.

The Hume-Rothery rules states that if there is a large enough difference in size and electronegativity between two atomic species, chemical order will be preferred, whereas for no or small differences disorder is favoured.⁵⁰ Our results indi-

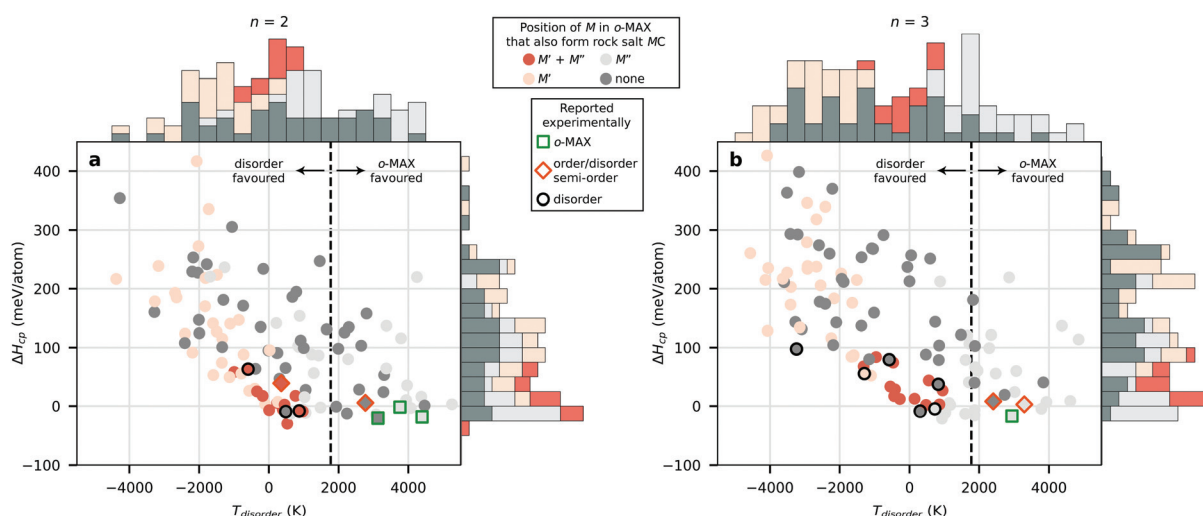


Fig. 7 Calculated formation enthalpy ΔH_{cp} as function of the disorder temperature $T_{disorder}$ for o-MAX phases with (a) $n = 2$ and (b) $n = 3$. The colours represent if the M' and/or M'' in o-MAX also forms rock salt MC. Experimentally reported phases are marked according to their reported order; green squares (o-MAX), black circles (disordered MAX), and orange diamonds (o-MAX, semi-order, or disorder). The vertical dashed line indicates the typical bulk synthesis temperature 1773 K.



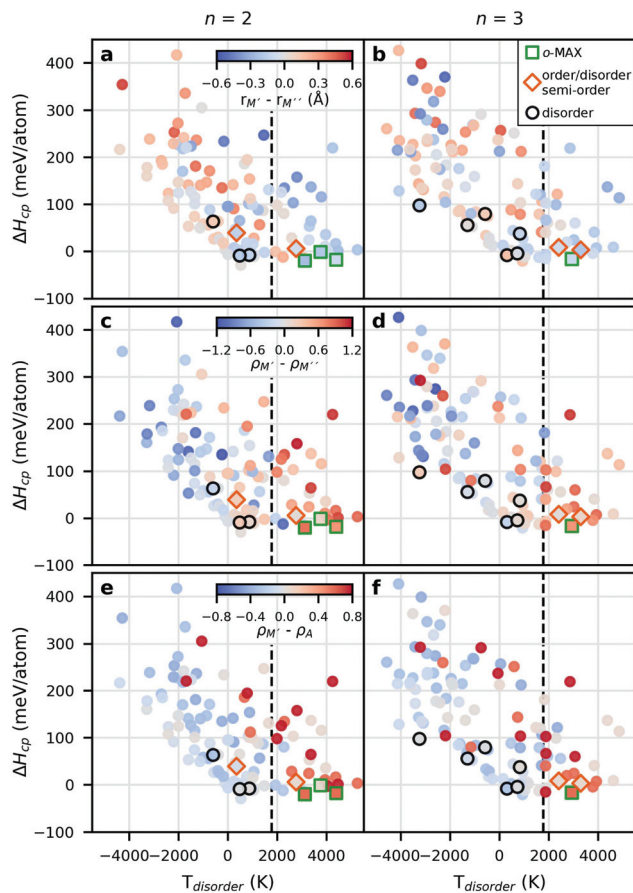


Fig. 8 Calculated formation enthalpy ΔH_{cp} for order of type A, o-MAX, as function of the disorder temperature $T_{disorder}$ for (a, c and e) M'_2M'' AlC_2 and (b, d and f) $M'_2M''_2AlC_3$. The colouring represents the difference between M' and M'' in (a and b) metallic radius r and (c and d) electronegativity ρ . In (e and f) the colouring represents the difference in electronegativity between M' and Al. Experimentally reported phases are marked according to their reported order; green squares (o-MAX), black circles (disorder MAX), and orange diamonds (o-MAX, semi-order, or disorder). The vertical dashed line indicates a typical bulk synthesis temperature of 1773 K.

cate that an explanation for order/disorder formation upon alloying between M' and M'' within the 312 and 413 MAX phase structure is only consistent with the part of the Hume-Rothery rules related to electronegativity. When it comes to the size criteria for ordering, we find that a large size difference of M' and M'' within order of type A (o-MAX) is detrimental, with $T_{disorder} < 0$ in general and $\Delta H_{cp} \gg 0$. This is most pronounced for Y-based phases due to its large metallic radius (1.80 Å), which results in compressive stress in the Y-layers while the layers with smaller atoms will be under tensile stress. This is opposite to the in-plane ordered i-MAX phases,^{18,19,21–23} related to the 211 MAX phases, where a significant size difference between M' and M'' is required for the ordered formation of M' and M'' in a 2 : 1 ratio within each M-layer.

Based on herein presented result we propose guidelines for which M combination to use when targeting either chemical order (out-of-plane) or disorder in 312 and 413 MAX phases.

Stable phases with preference for chemical order at typical bulk synthesis temperatures have mainly been identified for systems where the central M'' , sandwiched by C, also form rock-salt MC and with $M' = Cr$ and Mo next to the Al-layer. This is most pronounced for the 413 system but is also valid for the 312 systems. For the 312 systems we have also identified ordered phases with $M' = Sc$ next to the Al-layer. o-MAX is mainly preferred when M' from group 6 (Cr, Mo, W) is combined with M'' from groups 4 and 5 (Ti, Zr, Hf, V, Nb, Ta). Disorder of M' and M'' is preferred when alloying metals from groups 3 to 5 (Sc, Ti, Zr, Hf, V, Nb, Ta).

A comparison of herein presented results with experimentally reported phases with order and/or disorder illustrates that ordered o-MAX phases can all be found within the region where we suggest that order is preferred, *i.e.*, $T_{disorder} > 1773$ K, while disordered MAX is found for $T_{disorder} < 1773$ K. Some M' and M'' combinations have been reported both as ordered and disordered, *e.g.*, $Cr_2V_2AlC_3$ and $(Cr_{0.5}V_{0.5})_4AlC_3$ (choice of notation indicating order/disorder), which have been reported as o-MAX with some degree of intermixing between the two M-sites and as disordered.^{17,48} We have previously shown that o-MAX phases can be stable both upon limited intermixing of M' and M'' , and at off-stoichiometries.^{15,24} Ti_2ZrAlC_2 or $(Ti_{0.67}Zr_{0.33})_3AlC_2$ is another example where both order^{45,49} and disorder^{42,51} have been claimed. Our results indicate that Ti and Zr prefer disorder or possibly semi-order, based on the moderate $T_{disorder} = 357$ K combined with a similar electronegativity of Ti and Al. It should be noted that within this study, only out-of-plane order have been considered, where each M-layer only consists of one elemental type only. Off-stoichiometries for o-MAX have been demonstrated both experimentally and theoretically, and shows that deviation from the ideal o-MAX composition is possible while still retaining the overall chemical order.^{15,17,24} Impact from off-stoichiometries, intermixing between M' and M'' layers, and vacancies at M, Al or C sites have previously been demonstrated for a few M' and M'' combinations to have minor influence on the qualitative results.²⁴ The possibility of in-plane order of M' and M'' , similar to i-MAX phases,^{18,19} in higher order MAX phases, 312 and 413, is beyond the scope of this work and a topic for future studies.

There are already MXenes realized from o-MAX phases^{16,25} and the range of materials predicted in the present work suggest that the number of chemically ordered as well as disordered MXenes, from o-MAX or solid solution 312 and 413 MAX phases, respectively, can be increased. This allows tuning of the MXene chemistry through one or two metals in the outmost surface layers, and alteration of fundamental properties through choice of metal embedded within in the MXene.

Conclusion

In conclusion, the present study demonstrates that formation of chemically ordered o-MAX phases is mainly governed by



having a M' (the metal layer closest to the A-layer) that do not form rock-salt MC and with an electronegativity larger than Al. Preference for chemical disorder is achieved when the difference in size and electronegativity of M' and M'' is small combined with minor differences in electronegativity of M' and Al. Through a systematic theoretical study of phase stability of quaternary MAX phases upon alloying between M' and M'' from groups 3 to 6 (Sc, Y, Ti, Zr, Hf, V, Nb, Ta, Cr, Mo, and W) in 312 (M'₂M''AlC₂ composition) and 413 (M'₂M''₂AlC₃ composition) structures, we confirm all synthesized phases to date with chemical order or disorder, and identify 7 stable (10 close to stable) hypothetical o-MAX phases, and 38 MAX phases with preference for disorder. These phases remain to be verified, and synthesis experiments are encouraged. We also propose guidelines for which M' and M'' combinations to use in search for chemically ordered o-MAX; M' from group 6 (Cr, Mo, W) together with M'' from groups 3–5 (Sc, Ti, Zr, Hf, V, Nb, Ta). Correspondingly, disordered MAX phases are obtained by combining M' and M'' within groups 3–5 (Sc, Ti, Zr, Hf, V, Nb, Ta). This study shows that adding a fourth element to form ordered and disordered quaternary MAX phases allows novel elemental combinations, in materials not yet synthesized, for potentially tuneable and advantageous properties. Moreover, based on o-MAX phases as parent materials for corresponding MXenes, we also expect that the range of attainable MXene compositions will be expanded.

Conflicts of interest

There are no conflicts of interest to declare.

Acknowledgements

J. R. acknowledge support from the Knut and Alice Wallenberg (KAW) Foundation for a Fellowship Grant and Project funding (KAW 2015.0043), and from the Swedish Foundation for Strategic Research (SSF) for Project Funding (EM16-0004). The Swedish Research Council is also gratefully acknowledged through Project 642-2013-8020. The calculations were carried out using supercomputer resources provided by the Swedish National Infrastructure for Computing (SNIC) at the National Supercomputer Centre (NSC), the High Performance Computing Center North (HPC2N), and the PDC Center for High Performance Computing.

Notes and references

- W. Jeitschko, H. Nowotny and F. Benesovsky, *Monatsh. Chem.*, 1963, **94**, 672–676.
- W. Jeitschko, H. Nowotny and F. Benesovsky, *Monatsh. Chem.*, 1964, **95**, 178–179.
- M. W. Barsoum and T. El-Raghy, *J. Am. Ceram. Soc.*, 1996, **79**, 1953–1956.
- M. W. Barsoum, *Prog. Solid State Chem.*, 2000, **28**, 201–281.
- M. Naguib, M. Kurtoglu, V. Presser, J. Lu, J. Niu, M. Heon, L. Hultman, Y. Gogotsi and M. W. Barsoum, *Adv. Mater.*, 2011, **23**, 4248–4253.
- M. Naguib, V. N. Mochalin, M. W. Barsoum and Y. Gogotsi, *Adv. Mater.*, 2014, **26**, 992–1005.
- B. Anasori, M. R. Lukatskaya and Y. Gogotsi, *Nat. Rev. Mater.*, 2017, **2**, 16098.
- F. Shahzad, M. Alhabeab, C. B. Hatter, B. Anasori, S. Man Hong, C. M. Koo and Y. Gogotsi, *Science*, 2016, **353**, 1137–1140.
- F. L. Meng, Y. C. Zhou and J. Y. Wang, *Scr. Mater.*, 2005, **53**, 1369–1372.
- T. Cabioch, P. Eklund, V. Mauchamp, M. Jaouen and M. W. Barsoum, *J. Eur. Ceram. Soc.*, 2013, **33**, 897–904.
- A. S. Ingason, A. Mockute, M. Dahlqvist, F. Magnus, S. Olafsson, U. B. Arnalds, B. Alling, I. A. Abrikosov, B. Hjörvarsson, P. O. Å. Persson and J. Rosen, *Phys. Rev. Lett.*, 2013, **110**, 195502.
- V. Saltas, D. Horlait, E. N. Sgourou, F. Vallianatos and A. Chroneos, *Appl. Phys. Rev.*, 2017, **4**, 041301.
- Z. Liu, E. Wu, J. Wang, Y. Qian, H. Xiang, X. Li, Q. Jin, G. Sun, X. Chen, J. Wang and M. Li, *Acta Mater.*, 2014, **73**, 186–193.
- B. Anasori, J. Halim, J. Lu, C. A. Voigt, L. Hultman and M. W. Barsoum, *Scr. Mater.*, 2015, **101**, 5–7.
- B. Anasori, M. Dahlqvist, J. Halim, E. J. Moon, J. Lu, B. C. Hosler, E. N. Caspi, S. J. May, L. Hultman, P. Eklund, J. Rosén and M. W. Barsoum, *J. Appl. Phys.*, 2015, **118**, 094304.
- R. Meshkian, Q. Tao, M. Dahlqvist, J. Lu, L. Hultman and J. Rosen, *Acta Mater.*, 2017, **125**, 476–480.
- E. N. Caspi, P. Chartier, F. Porcher, F. Damay and T. Cabioch, *Mater. Res. Lett.*, 2015, **3**, 100–106.
- Q. Tao, M. Dahlqvist, J. Lu, S. Kota, R. Meshkian, J. Halim, J. Palisaitis, L. Hultman, M. W. Barsoum, P. O. Å. Persson and J. Rosen, *Nat. Commun.*, 2017, **8**, 14949.
- M. Dahlqvist, J. Lu, R. Meshkian, Q. Tao, L. Hultman and J. Rosen, *Sci. Adv.*, 2017, **3**, e1700642.
- L. Chen, M. Dahlqvist, T. Lapauw, B. Tunca, F. Wang, J. Lu, R. Meshkian, K. Lambrinou, B. Blanpain, J. Vleugels and J. Rosen, *Inorg. Chem.*, 2018, **57**, 6237–6244.
- M. Dahlqvist, A. Petruhins, J. Lu, L. Hultman and J. Rosen, *ACS Nano*, 2018, **12**, 7761–7770.
- R. Meshkian, M. Dahlqvist, J. Lu, B. Wickman, J. Halim, J. Thörnberg, Q. Tao, S. Li, S. Intikhab, J. Snyder, M. W. Barsoum, M. Yildizhan, J. Palisaitis, L. Hultman, P. O. Å. Persson and J. Rosen, *Adv. Mater.*, 2018, **30**, 1706409.
- J. Lu, A. Thore, R. Meshkian, Q. Tao, L. Hultman and J. Rosen, *Cryst. Growth Des.*, 2017, **17**, 5704–5711.
- M. Dahlqvist and J. Rosen, *Phys. Chem. Chem. Phys.*, 2015, **17**, 31810–31821.
- B. Anasori, Y. Xie, M. Beidaghi, J. Lu, B. C. Hosler, L. Hultman, P. R. C. Kent, Y. Gogotsi and M. W. Barsoum, *ACS Nano*, 2015, **9**, 9507–9516.



- 26 P. E. Blöchl, *Phys. Rev. B: Condens. Matter Mater. Phys.*, 1994, **50**, 17953–17979.
- 27 G. Kresse and D. Joubert, *Phys. Rev. B: Condens. Matter Mater. Phys.*, 1999, **59**, 1758–1775.
- 28 G. Kresse and J. Hafner, *Phys. Rev. B: Condens. Matter Mater. Phys.*, 1993, **47**, 558–561.
- 29 G. Kresse and J. Furthmüller, *Comput. Mater. Sci.*, 1996, **6**, 15–50.
- 30 G. Kresse and J. Furthmüller, *Phys. Rev. B: Condens. Matter Mater. Phys.*, 1996, **54**, 11169–11186.
- 31 J. P. Perdew, K. Burke and M. Ernzerhof, *Phys. Rev. Lett.*, 1996, **77**, 3865–3868.
- 32 H. J. Monkhorst and J. D. Pack, *Phys. Rev. B: Solid State*, 1976, **13**, 5188–5192.
- 33 Y. Ze-Jin, L. Rong-Feng, G. Qing-He, X. Heng-Na, X. Zhi-Jun, T. Ling, J. Guo-Zhu and G. Yun-Dong, *Sci. Rep.*, 2016, **6**, 34092.
- 34 M. Dahlqvist, R. Meshkian and J. Rosen, *Data Brief*, 2017, **10**, 576–582.
- 35 A. Zunger, S. H. Wei, L. G. Ferreira and J. E. Bernard, *Phys. Rev. Lett.*, 1990, **65**, 353–356.
- 36 M. Dahlqvist, B. Alling, I. A. Abrikosov and J. Rosén, *Phys. Rev. B: Condens. Matter Mater. Phys.*, 2010, **81**, 024111.
- 37 M. Dahlqvist, B. Alling and J. Rosén, *Phys. Rev. B: Condens. Matter Mater. Phys.*, 2010, **81**, 220102.
- 38 P. Eklund, M. Dahlqvist, O. Tengstrand, L. Hultman, J. Lu, N. Nedfors, U. Jansson and J. Rosén, *Phys. Rev. Lett.*, 2012, **109**, 035502.
- 39 A. S. Ingason, A. Petruhins, M. Dahlqvist, F. Magnus, A. Mockute, B. Alling, L. Hultman, I. A. Abrikosov, P. O. Å. Persson and J. Rosen, *Mater. Res. Lett.*, 2014, **2**, 89–93.
- 40 A. Mockute, M. Dahlqvist, J. Emmerlich, L. Hultman, J. M. Schneider, P. O. Å. Persson and J. Rosen, *Phys. Rev. B: Condens. Matter Mater. Phys.*, 2013, **87**, 094113.
- 41 A. Mockute, P. O. Å. Persson, F. Magnus, A. S. Ingason, S. Olafsson, L. Hultman and J. Rosen, *Phys. Status Solidi RRL*, 2014, **8**, 420–423.
- 42 E. Zapata-Solvas, M. A. Hadi, D. Horlait, D. C. Parfitt, A. Thibaud, A. Chronos and W. E. Lee, *J. Am. Ceram. Soc.*, 2017, **100**, 3393–3401.
- 43 M. Naguib, G. W. Bentzel, J. Shah, J. Halim, E. N. Caspi, J. Lu, L. Hultman and M. W. Barsoum, *Mater. Res. Lett.*, 2014, **2**, 233–240.
- 44 J. Halim, J. Palisaitis, J. Lu, J. Thörnberg, E. J. Moon, M. Precner, P. Eklund, P. O. Å. Persson, M. W. Barsoum and J. Rosen, *ACS Appl. Nano Mater.*, 2018, **1**, 2455–2460.
- 45 B. Tunca, T. Lapauw, O. M. Karakulina, M. Batuk, T. Cabioch, J. Hadermann, R. Delville, K. Lambrinou and J. Vleugels, *Inorg. Chem.*, 2017, **56**, 3489–3498.
- 46 Z. Liu, L. Zheng, L. Sun, Y. Qian, J. Wang and M. Li, *J. Am. Ceram. Soc.*, 2014, **97**, 67–69.
- 47 L. Zheng, J. Wang, X. Lu, F. Li, J. Wang and Y. Zhou, *J. Am. Ceram. Soc.*, 2010, **93**, 3068–3071.
- 48 Y. Zhou, F. Meng and J. Zhang, *J. Am. Ceram. Soc.*, 2008, **91**, 1357–1360.
- 49 R. Arróyave, A. Talapatra, T. Duong, W. Son and M. Radovic, *Mater. Res. Lett.*, 2018, **6**, 1–12.
- 50 W. Hume-Rothery, R. E. Smallman and C. W. Haworth, *The structure of metals and alloys*, The Institute of Metals, London, 1969.
- 51 S. V. Konovalikhin, S. A. Guda and D. Y. Kovalev, *Inorg. Mater.*, 2018, **54**, 953–956.

